## Article details

Arenas-Lago D., Abdolahpur Monikh F., Vijver M.G. & Peijnenburg W.J.G.M. (2019), Dissolution and aggregation kinetics of zero valent copper nanoparticles in (simulated) natural surface waters: Simultaneous effects of pH, NOM and ionic strength, Chemosphere 226: 841-850.
Doi: 10.1016/j.chemosphere.2019.03.190

Chemosphere 226 (2019) 841–850

Contents lists available at ScienceDirect

Chemosphere

journal homepage: www.elsevier.com/locate/chemosphere

# Dissolution and aggregation kinetics of zero valent copper nanoparticles in (simulated) natural surface waters: Simultaneous effects of pH, NOM and ionic strength

Daniel Arenas-Lago [a], Fazel Abdolahpur Monikh [a, *], Martina G. Vijver [a], Willie J.G.M. Peijnenburg [a, b]

[a] Institute of Environmental Sciences (CML), Leiden University, P.O. Box 9518, 2300 RA, Leiden, the Netherlands
[b] National Institute of Public Health and the Environment (RIVM), Center for Safety of Substances and Products, Bilthoven, the Netherlands

## HIGHLIGHTS

- DOC accelerate the dissolution of $Cu^0$ ENPs.
- 10 mM $Ca^{2+}/Mg^{2+}$ increase the dissolution of $Cu^0$ ENPs due to particle stability.
- 5 mg/L DOC block the 10 mM $Ca^{2+}/Mg^{2+}$ induced dissolution to $Cu^0$ ENPs.
- Dissolution/aggregation behavior of $Cu^0$ ENPs is different at different pH's.

## GRAPHICAL ABSTRACT

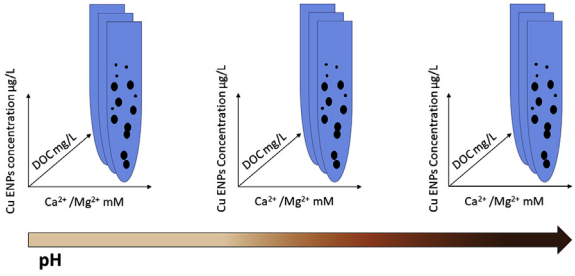


## ARTICLE INFO

*Article history:*
Received 27 December 2018
Received in revised form
22 March 2019
Accepted 31 March 2019
Available online 1 April 2019

Handling Editor: Petra Petra Krystek

*Keywords:*
Copper nanoparticles
Physico-chemical parameters
Natural water
Dissolution
Aggregation
Environmental fate
Complexation

## ABSTRACT

The combined effects of pH, dissolved organic carbon (DOC) and $Ca^{2+}/Mg^{2+}$ on the dissolution and aggregation kinetics of zero valent copper engineered nanoparticles ($Cu^0$ ENPs) were investigated. The dissolution and aggregation of the particles were studied in (a) synthetic aqueous media, similar in chemistry to natural surface waters, and (b) natural surface waters samples, for up to 32 or 24 h. The DOC stabilized the particles and prevented aggregation, and thus increased the available surface area. The higher available surface area in turn accelerated the dissolution of the particles. The presence of $Ca^{2+}/Mg^{2+}$, however, changed the aggregation and the dissolution of the DOC-stabilized particles. The influence of $Ca^{2+}/Mg^{2+}$ on DOC-stabilized particles was different at different pH's. In the absence of DOC, 10 mM of $Ca^{2+}/Mg^{2+}$ induced charge reversal on the particles and caused particle stability against aggregation. This subsequently increased particles dissolution. The results obtained with regard to dissolution and aggregation of the particles in natural surface waters were compared with those determined for the synthetic waters. This comparison showed that the behavior of the particles in the natural surface waters was mostly similar to the behavior determined for media at pH 9. Overall, the current study provides some novel insights into the simultaneous effects of physicochemical parameters of water on particle stability against aggregation and dissolution, and provides data about how the processes of aggregation and dissolution of $Cu^0$ ENPs interact and jointly determine the overall particle fate.



* Corresponding author. Van Steenis Building, Einsteinweg 2, 2333 CC, Leiden, the Netherlands.
*E-mail address:* f.a.monikh@cml.leidenuniv.nl (F. Abdolahpur Monikh).

https://doi.org/10.1016/j.chemosphere.2019.03.190
0045-6535/

## 1. Introduction

Many products containing engineered nanoparticles (ENPs) are currently on the market (Vance et al., 2015). Copper (Cu) ENPs are among the most commonly used ENPs with a wide range of applications, such as in electronics, textiles, ceramics, wood preservatives, inks, films and coatings, to name just a few of them (Vance et al., 2015). Upon production and application, Cu ENPs may enter the environment and end up in different environmental compartments such as natural surface water and sediment (Mudunkotuwa et al., 2012). Many studies nowadays focus on determining the fate and behavior of ENPs (Abdolahpur Monikh et al., 2018; Wagner et al., 2014), whereas only few data are available regarding the fate of Cu ENPs in the environment. In aquatic systems, the fate of Cu ENPs depends upon whether (a) the particles remain in dispersion, (b) processes that affect particle aggregation remove them from the water, or (c) dissolution changes their speciation (Johnson et al., 2011). Often these studies are limited to laboratory test conditions, although it is known that the natural conditions dramatically influence ENPs' environmental transformation and behavior (Conway et al., 2015). Understanding particle aggregation and dissolution kinetics under natural conditions is critical, since these processes have a decisive impact on the mobility and bioavailability of ENPs and, ultimately, on their toxicity in the aquatic environment (Li et al., 2012; Keller et al., 2010). Thus, dissolution/aggregation tests might be useful analytical tools for the regulatory assessment of not only Cu ENPs, but of dissolvable ENPs in general.

Literature showed that the dissolution kinetics of ENPs are influenced by particles aggregation and by physicochemical parameters of the system, such as ionic strength, pH and natural organic matter (NOM) (Keller et al., 2010; Flemming and Trevors, 1989). Aggregation of ENPs decreases the volume specific surface area of particles and subsequently reduces the dissolution of the particles (Zhang et al., 2010; Axson et al., 2015). For instance, it is reported that a decrease in the particle size of aggregates increases the dissolution rate of Cu ENPs (Adeleye et al., 2014) and silver (Ag) ENPs (Li et al., 2010a). Moreover, depending on their composition and the chemistry of the medium, NOM can stabilize (steric stabilization against aggregation) particles in suspension and through these mechanisms alter the dissolution rate and aggregation of ENPs (Conway et al., 2015; Wang et al., 2011). A decrease in the pH of an aquatic system may accelerate the dissolution of ENPs (Zhang et al., 2010). A study showed that at low pH, an elevated concentration of $Ca^{2+}$ increases the stability of titanium dioxide ($TiO_2$) ENPs against aggregation due to charge reversal of the particles (Von Der Kammer et al., 2010). Although many studies are available that investigated the effect of NOM, pH and ionic strength on aggregation and stability behavior of ENPs (Kanel et al., 2015; Chowdhury et al., 2013; Louie et al., 2015), the simultaneous influence of these parameters on the dissolution of ENPs is still not well known. The underlying mechanisms are not straightforward, particularly when it comes to the behavior of these particles under natural field conditions. For example, previous studies reported inconsistent results when investigating the effect of NOM on two types of zero valent ENPs, including $Ag^0$ ENPs (Gunsolus et al., 2015; Linlin and Tanaka, 2014; Linlin and Tanaka, 2014, 2014) and $Cu^0$ ENPs (Wang et al., 2015). Gunsolus et al. (2015) reported that NOM decreases the dissolution rate of $Ag^0$ ENPs, while Wang et al. (2015) reported that NOM increases the dissolution of $Cu^0$ ENPs. These contrasting reports created the motivation for this study to understand in greater detail the chemistry of NOM interactions with $Cu^0$ ENPs in simulated natural surface waters containing different pH and ionic strength, and to assess the dissolution rates and aggregation in dependence of the composition of the aqueous medium.

This study therefore first provides a large set of experimental data on dissolution and aggregation of $Cu^0$ ENPs in a model system mimicking natural surface waters (reported as synthetic media in this study) to systematically gain insight into how NOM, pH and ionic strength in conjunction influence aggregation and the dissolution of the particles in natural conditions. Second, the dissolution kinetics of $Cu^0$ ENPs are evaluated in samples from different natural surface waters by comparing the results obtained in these waters with the experimental data obtained from the synthetic media.

## 2. Material and methods

### 2.1. Chemicals and test materials

All chemicals were reagent grade and used without further purification unless noted. The water used was deionized by reverse osmosis and purified by a Millipore MilliQ (milliQ) system, making so-called milliQ water. Spherical bare $Cu^0$ ENPs with a nominal size of 25 nm, a purity of 99.5% and a specific surface area of 30–50 $m^2/g$ (according to the product information) were supplied from IoLiTec-Ionic Liquids Technologies GmbH. Optima grade hydrochloric acid (HCl, 30%) and nitric acid ($HNO_3$, 65%) were purchased from Merck (Suprapure®, USA). Sodium hydroxide (NaOH) was purchased from Sigma-Aldrich (Sigma-Aldrich Corp., St. Louis, MO, USA). Suwannee River NOM was supplied by the International Humic Substances Society (1R101 N).

### 2.2. Sampling areas and preparation of natural samples

The natural surface waters were collected from three different ditches, a lake (Valkenburgse Meer) and a river (Rijn) in the Netherlands (Fig. 1). Since the Ditches were shallow, to keep the sampling depth equal between all sampling area, the samples were collected from the first centimeters of the water column and brought to the laboratory of Leiden University on the same day. The physicochemical parameters of the samples (pH, concentration of NOM, concentration of $Ca^{2+}$ and concentration of $Mg^{2+}$) were measured and the samples were kept in a climate chamber under controlled conditions at 18 °C. After 24 h, the samples were filtered using a 0.45 μm Whatman filter paper and used for the experiment.

### 2.3. Characterization of the $Cu^0$ ENPs

The hydrodynamic size ($D_h$) and the zeta potential of the Cu particles in milliQ water and the natural samples were measured using a Zetasizer Nano device (Malvern Panalytical, Netherlands and UK). The morphology and size of the $Cu^0$ ENPs were also characterized by Transmission Electron Microscopy (JEOL 1010 TEM).

### 2.4. Preparation of synthetic water samples

The preparation of synthetic water samples containing NOM is described in Section 1 of the Supporting Information. The NOM was filtered (0.45 μm) and the filtered fraction, reported as dissolved organic carbon (DOC) in this study, was used. The stock DOC was used at four different concentrations, including 0, 5, 25, and 50 mg/L in milliQ water. Three concentrations of $CaCl_2$ and $MgSO_4$ were selected in a fixed content ratio of 4:1 ($Ca^{2+}/Mg^{2+}$) (the sum of 0, 2.5 and 10 mM $Ca^{2+}/Mg^{2}$). A ratio of 4:1 ($Ca^{2+}/Mg^{2+}$) simulates natural conditions, as reported by the OECD guidelines for stability testing of ENPs (Abdolahpur Monikh et al., 2018). To change the pH of the solution to three pH-levels ranging from 6 to 9, either 0.1 M NaOH or 0.1 M HCl was added. DOC served in these experiments as

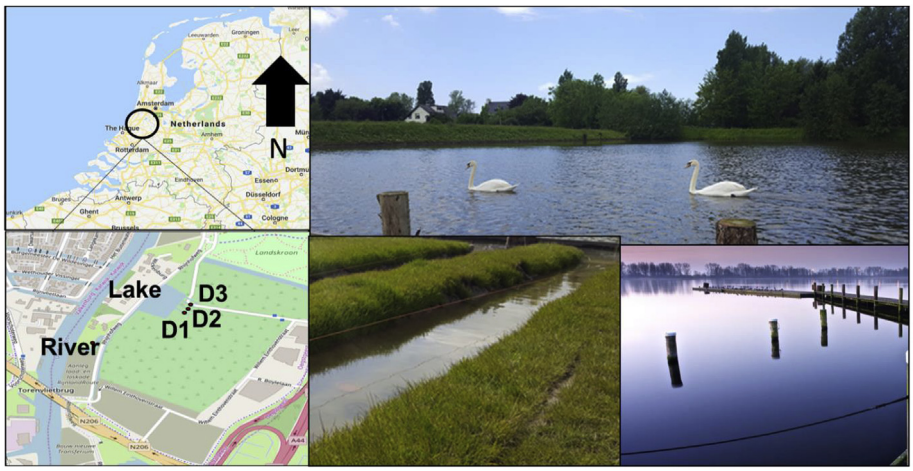


**Fig. 1.** Location of the sampling stations. D1: Ditch 1, D2: Ditch 2, D3: Ditch 3. The circle indicate the area where the sampling has been done.

a natural buffer to maintain a constant pH. The measured concentrations of DOC in the media with different conditions are reported in Tables 1–3 in the Supporting Information.

### 2.5. Developing the testing matrices

A stock suspension of $Cu^0$ ENPs (250 mg/L) was prepared in milliQ water and tip sonicated using a SONOPULS ultrasonicator (BANDELIN electronic. Berlin, Germany) at 100% amplitude for 10 min. To investigate the influence of pH, ionic strength and DOC content on the aggregation and dissolution behavior of $Cu^0$ ENPs, synthetic water samples were prepared using milliQ water. The different pH's, $Ca^{2+}/Mg^{2+}$ concentrations and DOC contents were selected according to the most common features of the waters reported by the Geochemical Atlas of Europe ("The Geochemical Atlas of Europe) and a previous study (Abdolahpur Monikh et al., 2018) to cover the variance of natural surface water conditions that is typical for European waters. From the sonicated stock dispersion, the required volume was added to reach a final concentration of 1 mg/L of $Cu^0$ ENPs in each testing medium. The dispersions were stored in a climate chamber under controlled conditions (20 ± 1 °C). All tests were performed in triplicate.

### 2.6. Aggregation kinetics

Aggregation kinetics were measured using dynamic light scattering (DLS). For measurement of $D_h$, dispersions (relevant for each testing medium) of 10 mg/L $Cu^0$ ENPs were sonicated at 100% amplitude for 10 min and immediately measured using DLS for 30 min. It was selected 10 mg/L only for $D_h$ measurement and not for exposure because measuring $D_h$ of 1 mg/L of ENPs using DLS is problematic due to size detection limit of the DLS. The measurements using DLS were carried out every 1 min; 30 data points in total for each samples.

**Table 2**
Physicochemical parameters of the samples collected from the natural surface water in the Netherlands.

| Sample | Cu (μg/L) | DOC (mg/L) | pH | Ca (mM) | Mg (mM) |
|---|---|---|---|---|---|
| Ditch 1 | < dl | 18.5 ± 1.3 | 9.0 ± 0.2 | 2.1 ± 0.7 | 1.2 ± 0.2 |
| Ditch 2 | < dl | 16.2 ± 1.6 | 8.9 ± 0.02 | " | " |
| Ditch 3 | < dl | 16.9 ± 1.3 | 9.2 ± 0.4 | " | " |
| Lake | < dl | 13.3 ± 1.8 | 8.6 ± 0.01 | 1.4 ± 0.4 | 0.76 ± 0.2 |
| River | < dl | 9.2 ± 1.3 | 7.67 ± 0.01 | 1.75 ± 0.1 | 9.0 ± 0.07 |

< dl: not detected, the concentration of Cu was lower than the detection limit of the instrument. "= same.

**Table 3**
Average dissolution rates ($k_{diss}$) of $Cu^0$ ENPs in the natural surface water samples up to 24 h.

| Sample | (ng $cm^{-2}$ $h^{-1}$) \| $R^2$ |
|---|---|
| Ditch 1 | 26.1 \| 0.99 |
| Ditch 2 | 23.6 \| 0.99 |
| Ditch 3 | 24.2 \| 0.98 |
| Lake | 21.2 \| 0.98 |
| River | 16.0 \| 0.98 |

### 2.7. Dissolution testing

Aliquots of the samples were taken immediately after preparation to measure the total copper concentration ($[Cu]_{total}$). To separate dissolved and particulate Cu, aliquots of each dispersion were

**Table 1**
Average dissolution rates ($k_{diss}$) of $Cu^0$ ENPs in the synthetic water samples up to 32 h.

| Concentration of $Ca^{2+}/Mg^{2+}$- DOC added | pH 6 (ng $cm^{-2}$ $h^{-1}$) \| $R^2$ | pH 7.5 (ng $cm^{-2}$ $h^{-1}$) \| $R^2$ | pH 9 (ng $cm^{-2}$ $h^{-1}$) \| $R^2$ |
|---|---|---|---|
| 0 mM–5 mg/L | | 17.1 \| 0.99 | 25.3 \| 0,92 |
| 0 mM–25 mg/L | | 28.7 \| 0.95 | 42.3 \| 0.99 |
| 0 mM–50 mg/L | | 27.5 \| 0.82 | 28.3 \| 0.97 |
| 2.5 mM–5 mg/L | 13.0 \| 0.58 | 23.0 \| 0.87 | 24.0 \| 0.97 |
| 2.5 mM–25 mg/L | 20.1 \| 0.60 | 31.2 \| 0.96 | 32.6 \| 0.95 |
| 2.5 mM–50 mg/L | 21.0 \| 0.68 | 22.0 \| 0.76 | 40.7 \| 0.96 |
| 10 mM–5 mg/L | | 13.1 \| 0.55 | 22.2 \| 0.92 |
| 10 mM–25 mg/L | | 17.4 \| 0.62 | 18.0 \| 0.85 |
| 10 mM–50 mg/L | | 11.0 \| 0,66 | 25.9 \| 0.83 |

taken at each time point (0, 4, 8, 24 and 32 h) and centrifuged at 4000 rpm for 30 min at 4 °C (Sorvall RC5Bplus centrifuge, Fiberlite F21-8). Samples were taken from the supernatant (top 5 cm), digested by $HNO_3$ and analysed for dissolved Cu ($[Cu]_{dissolved}$) using a flame atomic absorption spectrometer (FAAS; Perkin Elmer AAnalist 100). Changes in the $[Cu]_{dissolved}$ concentrations in the samples allow to examine the dissolution kinetics within 32 h of exposure.

### 2.8. Dissolution rate and its rate constant

The measured mass of $[Cu]_{dissolved}$ versus time was examined to obtain the dissolution rate constant following the approach reported by Levard et al. (2013). In this study, the rate constants were calculated for all conditions where the initial $[Cu]_{dissolved}/[Cu]_{total}$ at the first sampling time was less than 0.5. The samples with initial $[Cu]_{dissolved}/[Cu]_{total}$ higher than 0.5 were considered as being reflective of very fast dissolution conditions that could not be reliably assessed by means of the methods employed in this study. The data showed that, as expected, the dissolution rate was not constant across all water samples tested. The calculation of the dissolution rate constants was carried out assuming pseudo first-order kinetics.

### 2.9. Statistics and data analysis

Data were analysed statistically with the statistical program SPSS v. 19. Data are expressed as the average ± standard deviation (SD) of three replicates. Kolmogorov-Smirnov and Levene tests were applied to check the normality and homogeneity of variances, respectively, in order to test their homoscedasticity. ANOVA and Duncan's multiple range tests were used to compare the differences between groups ($p < 0.05$). An initial linear regression analysis was performed by fitting data on $[Cu]_{dissolved}$ versus time. The graphs were created by the software OriginLab 9.1.

## 3. Results and discussion

### 3.1. Characterization of $Cu^0$ ENPs

The $Cu^0$ ENPs were characterized in milliQ water immediately after sonication. The DLS data showed that the $Cu^0$ ENPs were well dispersed immediately after sonication. Rapid aggregation of the particles was however observed over time. After 1 h, the particle $D_h$ was between 278 nm and 425 nm (Table 4, Supporting Information). TEM microscopy confirmed the intense aggregation of the particles in milliQ water immediately after sonication (Fig. 1, Supporting information). An averaged zeta potential value of about $-3.4 \pm 0.4$ mV was measured by electrophoretic mobility. The point of zero charge (PZC) for $Cu^0$ ENPs from alkalimetric titration was at pH of 8.5–9 and close to previously reported values for similar particles (Collins et al., 2012; Kosmulski, 2009).

### 3.2. Particle aggregation behavior in synthetic water

The aggregation kinetics of $Cu^0$ ENPs nanoparticles were investigated over DOC, $Ca^{2+}/Mg^{2+}$ and pH ranges of 0–10 mM, 0–50 mg/L, and 6–9 respectively. The Polydispersity Index (PDI) was in the range of 0.02–0.48 for all the measurements. At pH 6, the trends in the patterns of aggregation over time were similar in almost all conditions (Fig. 2). Immediate aggregation in the first few minutes (up to 10 min) in the media without DOC and 0–2.5 mM $Ca^{2+}/Mg^{2+}$ was typically observed. A downward trend in aggregate size from 0 to 30 min was observed in some media. This trend was likely due to sedimentation of the largest aggregates (Conway et al., 2015) and due to fast dissolution of the particles. At pH 7.5, the particles showed a typical increase in sizes over time in the media without DOC and $Ca^{2+}/Mg^{2+}$. At pH 9, substantial aggregation was observed for media without DOC and at $Ca^{2+}/Mg^{2+}$ concentrations of 0 and 2.5 mM.

### 3.3. Particle dissolution behavior in synthetic waters

The concentrations of Cu ions (μg/l) were measured in the supernatant (top 5 cm) during 32 h of incubation in the synthetic media. The ratio of $[Cu]_{dissolved}/[Cu]_{total}$ was calculated and plotted as a function of exposure time for the different media at pH 6, 7.5 and 9. The data show a good reproducibility, with generally low variations between the replicates.

As shown in Fig. 3, in almost all media the final amount (at 32 h) of $[Cu]_{dissolved}$ in the supernatant increased as compared to the initial concentration, except for the media contain 0 or 2.5 mM $Ca^{2+}/Mg^2$ and 0 mg/L DOC at pH 9 (Fig. 3C). When introduced into the water, $Cu^0$ ENPs were immediately oxidized, as previously reported (Collins et al., 2012; Conway et al., 2015). This resulted in an immediate increase in the concentration of $[Cu]_{dissolved}$ in the suspension at the first sampling time (measurement at exactly 0 h was not possible given the time needed for sample preparation, including sonication, centrifugation, etc.) and continued to increase up to 32 h. The dissolution over time was different across the different media. The initial concentrations of $[Cu]_{dissolved}$ in the media without DOC and without addition of $Ca^{2+}/Mg^2$ were higher at pH 6 than at pH 7.5 and 9, whereas the concentration of $[Cu]_{dissolved}$ increased slightly at pH 6 during 32 h. As described by Wang et al. (2016), the dissolution of $Cu^0$ ENPs in water is an oxidative process following the stoichiometry below (eq. (1)):

$$Cu^0(s) + 1/4\ O_2\ (aq) + H^+\ (aq) \leftrightarrow Cu^+\ (aq) + 1/2\ H_2O \quad (1)$$

According to this stoichiometry, oxygen and $Cu^+$ are the factors controlling the dissolution of the particles in the system. When $Cu^0$ ENPs are dispersed in a solution containing dissolved oxygen, release of Cu ions is observed (Zou et al., 2017). Dissolution may continue for a long time, but eventually the $[Cu]_{dissolved}$ concentration typically reaches a plateau. Once the system has reached a state of equilibrium, the particles may persist dissolution even in the presence of free oxygen (Molleman and Hiemstra, 2017). This stability could be attributed to the formation of a layer of Cu oxide (CuO and $Cu_2O$) on the surface of the particles (Mudunkotuwa et al., 2012). However, Cu oxide is highly soluble and will generally not be stable for a long time under different physicochemical conditions. At neutral and acidic pH, the solubility of Cu oxide is some orders of magnitudes higher than at pH > 8, which limits the persistence of a Cu oxide layer on the surface of the particles (Mudunkotuwa et al., 2012). This could explain the higher stability observed at pH 9 in comparison to the stability at pH ≤ 7.5. Similar results were reported by Jones and Su (2012) for dissolution of $Cu^0$ ENPs as a function of pH, and Molleman and Hiemstra (2017) for dissolution of Ag oxide formed on the surface of Ag ENPs. In the latter study the authors reported that formation and persistence of Ag is highly unlikely, unless the pH is very high.

In the absence of DOC, the concentration of dissolved Cu decreased after 4 h of exposure at all pH values, except for media containing 10 mM $Ca^{2+}/Mg^2$ at pH 6 and 7.5 (Figs. 3a and 1b). This decrease can be attributed to re-precipitation of $Cu^{2+}$ on the surface of the $Cu^0$ ENPs (Jones and Su, 2012) as reported for Ag ENPs by Levard et al. (2013). The final concentrations of $[Cu]_{dissolved}$ in the media without DOC were also lower than those in media treated with DOC, except in the presence of 10 mM $Ca^{2+}/Mg^{2+}$. This may result from the fast aggregation of particles which took place as the

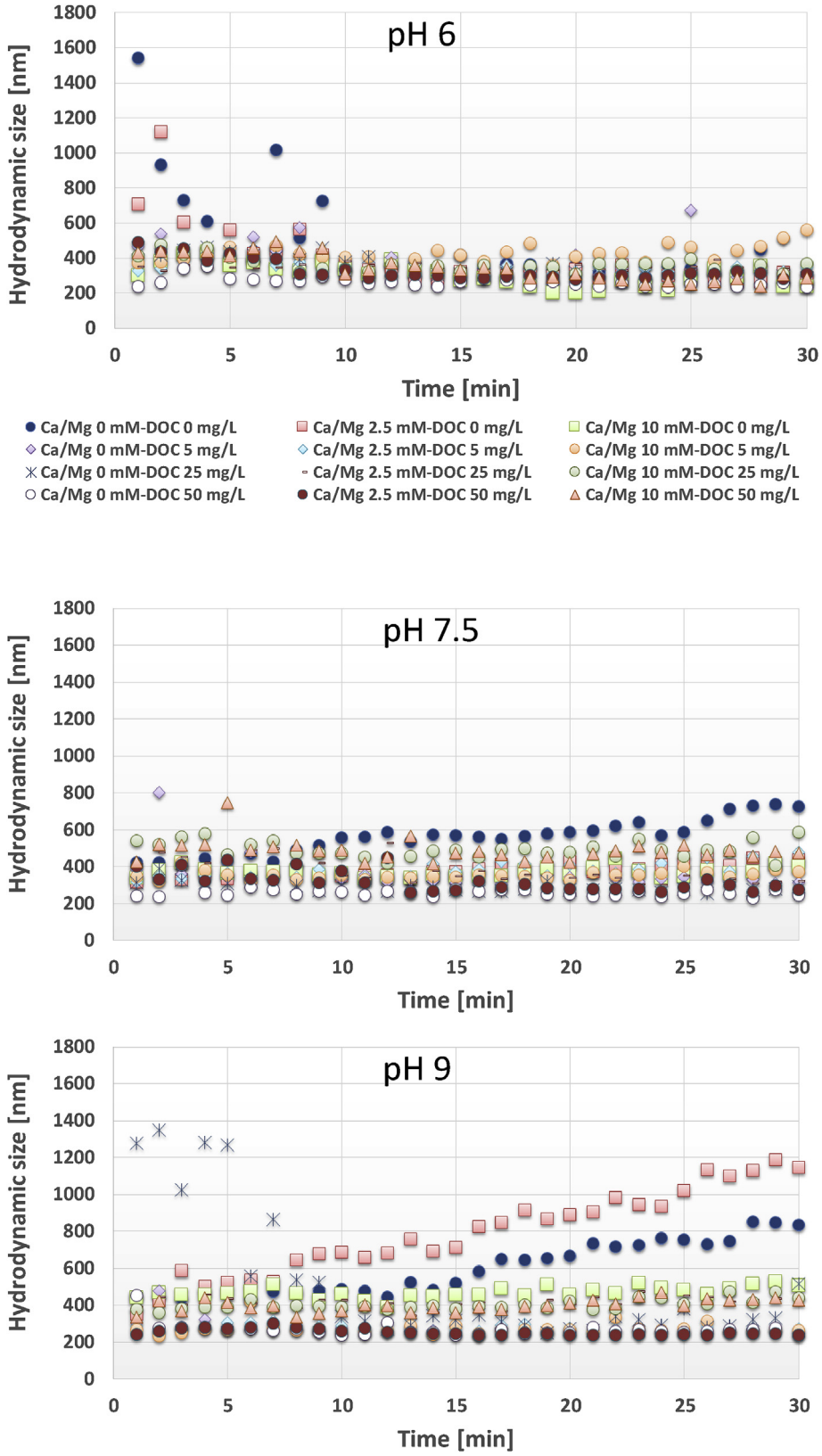


**Fig. 2.** Aggregation kinetics of $Cu^0$ ENPs as a function of DOC concentration, ionic strength and pH over 30 min of measurement using DLS.

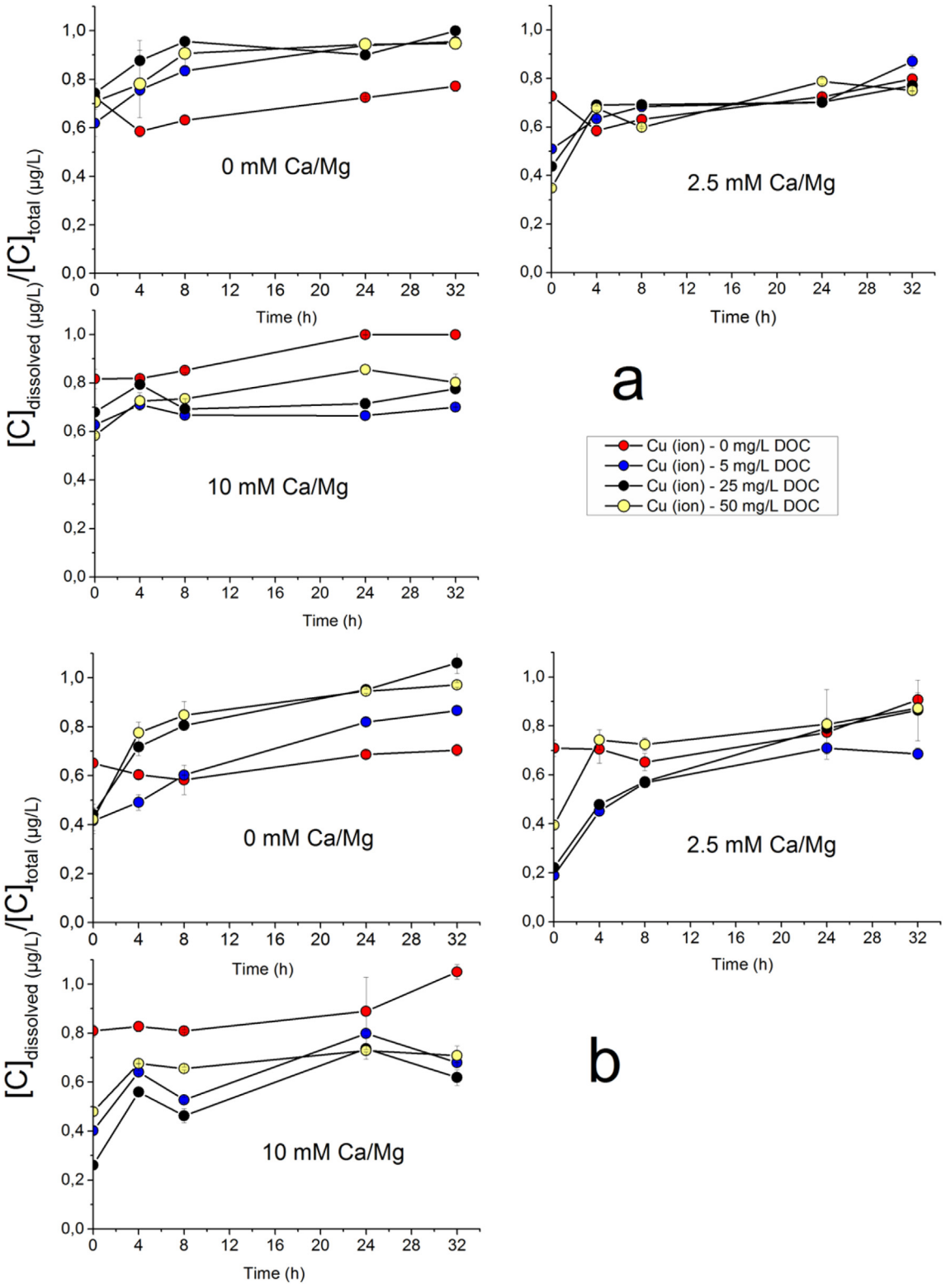


**Fig. 3.** Dissolved copper fraction and standard deviation after 32 h of exposure of $Cu^0$ ENPs under various DOC and $Ca^{2+}/Mg^{2+}$ concentration (Millimoles) at (a) pH 6, (b) pH 7.5 and (c) pH 9 in the synthetic media. The total electrolyte concentration is expressed as Millimoles (mM).

particles were introduced in the media without DOC. This results in a lower available surface area and, subsequently, lower dissolution kinetics as reported by Li et al. (2010a,b). The aggregation results confirmed these observations (Fig. 2). Similar results were previously reported for Cu ENPs as aggregation was found to decrease the ion release from the particles (Adeleye et al., 2014).

The presence of $Ca^{2+}/Mg^{2+}$ in the media accelerated the aggregation of the particles, which is in line with the Derjaguin Landau Verwey Overbeek (DLVO) theory. Enhanced aggregation is due to compression of the diffuse double electrical layer of $Cu^0$

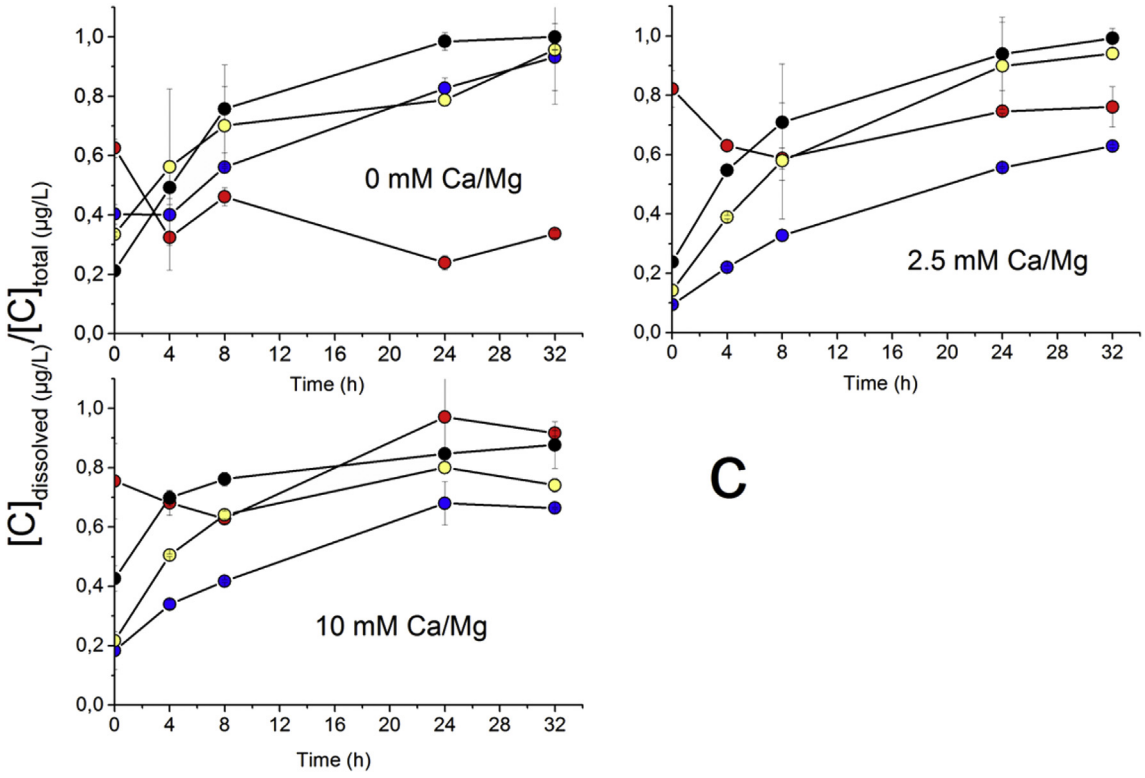


**Fig. 3.** (*continued*).

ENPs. However, in the media containing 10 mM $Ca^{2+}/Mg^{2+}$ and pH lower that 8, the particles were stable against aggregation and the rate of dissolution was high, in some cases even higher than in case of DOC-induced dissolution (Fig. 3). This finding also was in agreement with the zeta potential of the particles (Table 5, Supporting Information). At pH < 7.5 and without DOC, the particles are positively charged (Table 5, Supporting Information). An increase in the concentration of $Ca^{2+}/Mg^{2+}$ increases the positive charge of the particles due to specific interactions of $Ca^{2+}$ ions with the particles (Abdolahpur Monikh et al., 2018). This results in a high positive zeta potential. This thick double layer reduces the successful collision between particles, which in turn will decrease the aggregation rate. Consequently the particles remain stable against aggregation for a longer period of time and dissolution increases.

In agreement with previous studies (Wang et al., 2011, 2015), the presence of DOC increases the amount of dissolved Cu (Fig. 3). In the presence of DOC and absence of $Ca^{2+}/Mg^{2+}$, the particles remain stabilized in the suspension and do not aggregate. This leads to a high dissolution rate of the particles. NOM can act as a ligand that effectively interacts with Cu ENPs (Wang et al., 2015). NOM induces both a negative surface charge and steric stabilization on the surface of $Cu^0$ ENPs due to the interaction of carboxylic and phenolic functional groups with the particle surface. This could stabilize the particles electrostatically and sterically against aggregation (Jones and Su, 2012). In the presence of high concentrations of DOC, a higher amount of functional groups are available to form strong complexes with the $Cu^0$ ENPs. The complexation of DOC with Cu ENPs (with CuO and $Cu_2O$ present on the surface of the particles) weakens the surface Cu–Cu and Cu–O bonds (Korshin et al., 1998; Aiken et al., 2011; Wang et al., 2015), which leads to enhanced dissolution through ligand promoted processes (Misra et al., 2012). Dissolved Cu ions, independent of their release being induced by DOC, protons and/or hydroxide ions, have a greater affinity towards organic ligands to form insoluble complexes with DOC (Mudunkotuwa et al., 2012). Thus, after release, Cu ions can form strong complexes with the functional groups of DOC via intra- or intermolecular bidentate chelation (Wang et al., 2015). If the concentration of DOC in the system is high, the Cu concentration gradient between the particle surface and the functional groups acts as the driving force of particle dissolution, resulting also in a decrease of the mineral saturation index (the driving force for precipitation) (Aiken et al., 2011).

At pH 6 (Figure 3a) and 0 mM $Ca^{2+}/Mg^{2+}$, there was no significant difference in the dissolution patterns of $Cu^0$ ENPs between media containing 5, 25 and 50 mg/L DOC. The same results were observed in the media with 2.5 mM $Ca^{2+}/Mg^{2+}$. However, in the presence of 10 mM $Ca^{2+}/Mg^{2+}$, the highest and the lowest extent of dissolution were observed in the media containing 50 and 5 mg/L DOC, respectively. These results indicate that at a high concentration of $Ca^{2+}/Mg^{2+}$, 5 mg/L DOC blocks the enhancement in the positive charge on the surface of the particles due to specific interaction of $Ca^{2+}$ with particles, but also was not able to stabilize the particles against aggregation. Thus, the particles underwent aggregation, which led to a decrease in the dissolution rate.

At pH 7.5 (Fig. 3b) and pH 9 (Fig. 3c), the influence of DOC on the dissolution of the $Cu^0$ ENPs decreases as the concentration of $Ca^{2+}/Mg^{2+}$ increases in the media. The differences between media containing different DOC concentrations are also more pronounced in comparison to those at pH 6. At pH ~ 9, the zeta potential is close to zero and the particles are unstable and may aggregate relatively easy to form large particles. The larger aggregates influence the rate of release of ions in the media and the final $[Cu]_{dissolved}$ at 32 h. Previous studies also reported that dissolution of Cu ENPs (Adeleye et al., 2014) and Zn ENPs (Odzak et al., 2014) decreases as the pH of the system increases. Griffitt et al. (2007) reported that less than 0.1% of Cu ENPs dissolved in media at pH 8.2 after 48 h. However, the dissolution increased to 98% Cu ENPs at pH 6 after one week. Overall, the observation of higher rates of dissolution of the

particles in the presence of DOC compared to the rates of dissolution in the absence of DOC shows that even (a) the presence of high levels of $Ca^{2+}/Mg^{2+}$ in the media, which can increase the aggregation and reduce the available surface area, and (b) the formation of Cu oxides on the surface of $Cu^0$ ENPs at high pH values cannot overcome the DOC promoted dissolution of the particles. The interaction Cu-DOC-carboxylic groups is predominantly covalent, outweighing the electrostatic effect of $Ca^{2+}/Mg^{2+}$, and at higher pH the polyionic DOC colloid is highly negatively charged, thus facilitating covalent bonding with $Cu^{2+}$.

### 3.4. Dissolution rate in synthetic water

The dissolution rates ($k_{diss}$) of the $Cu^0$ ENPs, determined from the slopes of the $[Cu]_{dissolved}$ versus time, for synthetic waters are reported in Table 1. Very fast dissolution and high values of $k_{diss}$ were observed in some samples at rates that were too high to be assessed by means of the methods used in this study. No numerical values for the rate constants are included in Table 1 for these samples. As reported in Table 1, the $k_{diss}$ differed between the media tested. At pH 6 and $Ca^{2+}/Mg^{2+}$ concentration of 2.5 mM, increases in the concentration of DOC increased the $k_{diss}$ of $Cu^0$ ENPs dissolution. A similar trend was observed at pH 9 for sample containing 2.5 mM $Ca^{2+}/Mg^{2+}$. Furthermore, the apparent $k_{diss}$ of the particles increased as the pH value increased from 6 to 9 (Table 1). This is contradictory to what one would expect on the basis of eq (1) which could be due to the combined effects of pH, $Ca^{2+}/Mg^{2+}$ and DOC. The $k_{diss}$ of the $Cu^0$ ENPs in the samples containing no $Ca^{2+}/Mg^{2+}$ were higher compared to those in media containing 2.5 and 10 mM. The differences in the release behavior were discussed in the previous section. These results suggest that the rate of dissolution of ENPs is strongly dependent on the concentration of DOC and the pH of the media as reported in previous studies (Mitrano et al., 2014; Molleman and Hiemstra, 2017). It must be also mentioned that aggregation affects the $k_{diss}$, especially for the high ionic strength suspensions. This explains the lower $k_{diss}$ observed in high ionic strength media.

### 3.5. Particle dissolution behavior in natural surface waters

The physicochemical parameters of the samples collected from five different natural surface waters in the Netherlands were measured and reported in Table 2. The background concentration of Cu in the samples was lower than the detection limit of the instrument (<1 ppb). The concentration of DOC was between 9.2 and 18.5 mg/L with the highest concentration measured in Ditch 1 followed by Ditch 3 ≥ Ditch 2 > Lake > River. The highest pH value was recorded for Ditch 1 and the lowest was recorded in the River. The pH of all samples was in the neutral – slightly basic range and exceeded 7.6. According to the data reported in the Geochemical Atlas of Europe the highest concentration of $Ca^{2+}$ and $Mg^{2+}$ are 4,12 and 1,06 mM respectively. From these results is may be deduced that the conditions in the natural waters sampled are mostly mimicked by the synthetic media contain 5–20 mg/L DOC, 2.5–10 mM of $Ca^{2+}/Mg^{2+}$ and 7.5–9 pH.

The $[Cu]_{dissolved}$ of $Cu^0$ ENPs was determined in the natural surface waters (Fig. 4). After 24 h, the $[Cu]_{dissolved}$ in water followed this order; Ditch 1 > Ditch 2 > Ditch 3 ≥ Lake > River. The concentration of DOC in the Ditches and Lake is higher than that in the River. The results, thus, also imply that a higher extent of dissolution of $Cu^0$ ENPs in the Ditches and in the Lake than in the River is likely to occur. According to these results, it is likely that DOC-enhanced dissolution of $Cu^0$ ENPs is occurring in the natural waters, as observed in the synthetic waters. One should also consider that the physicochemical parameters of natural surface waters are changing dramatically from place to place and season to season. Thus, these variations will modify the dissolution and aggregation behavior of the particles dramatically. The reported data herein are therefore to be considered a snapshot of what occurs under dynamic natural conditions. The rate constants measured in the natural samples provide a general overview of the range of dissolution/aggregation of $Cu^0$ ENPs in natural conditions and show that the rate constants obtained in synthetic waters are indeed comparable to the rate constants in natural waters of similar compositions. Natural systems are inherently complex, which makes it difficult to directly compare the data with other published studies. Mitrano et al. (2014) reported that for most circumstances, the $k_{diss}$ of Ag ENPs was higher in water originating from a creek as compared to the $k_{diss}$ in distilled water and in tap water. It must be mentioned that chloride, $Cl^-$, which is a common ligand in natural surface waters, may form a complex with Cu ENPs or with Cu ions released during particle oxidation, and thus may influence the

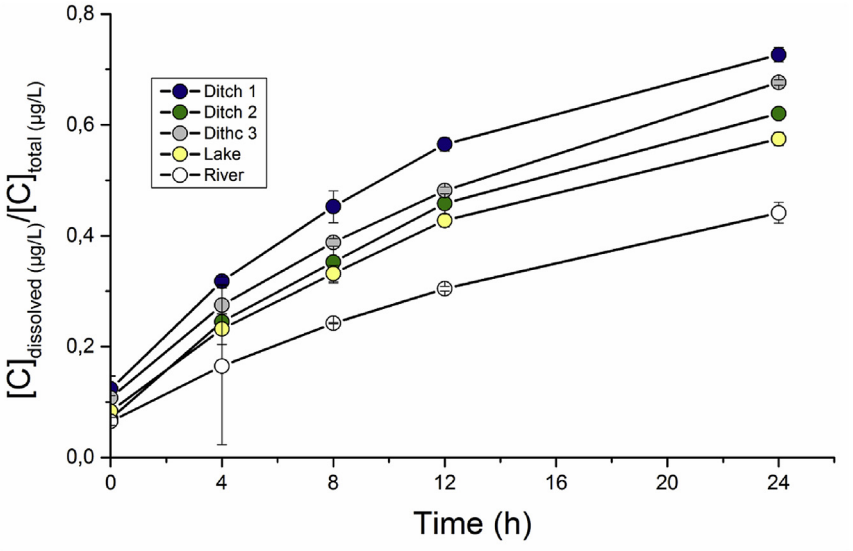


**Fig. 4.** Dissolved copper fraction and standard deviation over 24 h in natural surface water collected from the Netherlands.

dissolution rate of the particles (Levard et al., 2011; Mitrano et al., 2014). In this research, the influence of $Cl^-$ was not investigate and this could be a motivation for future studies in which the impact of $Cl^-$ on particle dissolution is explicitly considered.

Measuring $D_h$ using DLS to determine the aggregation kinetics of ENPs in natural water is challenging due to the limitation of the technique to deal with samples containing different natural particles (von der Kammer et al., 2012). In addition, it was noticed that there were natural particles settlements in the cuvettes which led to particle sedimentation as a consequence of heteroaggregation. Thus, reliably measuring the $D_h$ using DLS to obtain the aggregation kinetics of $Cu^0$ ENPs in natural samples was not possible in this study. The measured zeta potential values are reported in Table 6 in the Supporting information.

As can be seen in Fig. 4, a slightly higher extent of dissolution than in any of the other waters was observed for Ditch 1. The second highest $[Cu]_{dissolved}$ was observed in Ditch 3, followed by Ditch $2 \geq$ Lake > River. The concentration of $[Cu]_{dissolved}$ in the River sample was significantly lower than in the other natural waters samples. The initial level of $[Cu]_{dissolved}$ in all the natural waters, after addition of $Cu^0$ ENPs, was around 0.1 μg/L, which is similar to what was recorded for the synthetic media with 2.5 mM $Ca^{2+}/Mg^{2+}$ at pH 7.5 and 9.

The values of $k_{diss}$ as calculated for the natural samples are reported in Table 3. The $k_{diss}$ in the investigated natural waters was similar to that calculated for the synthetic media. The $k_{diss}$ in Ditch 1, 2 and 3 was higher that the lake and the river. The rate constant in the river was similar to the rate constant obtained for the synthetic medium containing 10 mM $Ca^{2+}/Mg^{2+}$, 5, 25 and 50 m/L DOC and pH 7.5. Considering the physicochemical parameters of the river (Table 2), this constant rate is expected for the river.

## 4. Conclusions

The key finding of this study is that dissolution and aggregation of $Cu^0$ ENPs are highly dependent on the DOC, ionic strength and pH of the aqueous media. DOC can induce dissolution of $Cu^0$ ENPs by controlling the aggregation, thus the available surface area, of the particles and by weakening the Cu–Cu and Cu–O bonds formed as a result of oxidation on the surface of the particles. Moreover, DOC can sorb the released Cu ions from the particles and, subsequently, accelerate the dissolution. Changes in the pH induced dissolution of the particles by causing instability of the copper oxide shell formed on the surface of the particles, as particularly observed in pH 6. The presence of $Ca^{2+}/Mg^{2+}$ also modified the dissolution behavior of $Cu^0$ ENPs by controlling the aggregation state of the particles and by interacting with functional groups available within the DOC. The impact of DOC on dissolution was stronger than the impacts of either $Ca^{2+}/Mg^{2+}$ (ionic strength) or pH.

In the case of the natural surface waters investigated in this study, similar trends of dissolution over time were determined with the highest and lowest concentrations of dissolved Cu in Ditch 1 and in the River water respectively. The dissolution behavior of the particles in the natural samples was most similar to the behavior determined for synthetic media containing 5–25 mg/L DOC, 2.5 and 10 mM $Ca^{2+}/Mg^{2+}$, and pH 9. These findings imply that DOC also controls the dissolution behavior of $Cu^0$ ENPs in natural waters given the similarity of the results obtained for synthetic media and those determined for natural samples. Our findings show that DOC-, pH- and ionic strength-driven dissolution/aggregation are important processes affecting the fate of $Cu^0$ ENPs in natural waters. This implies that the impact of these water properties on the fate of soluble ENPs needs to be investigated simultaneously rather than by means of separate tests in which each property is modified univariately. Bearing the results of this study in mind, it is to be concluded that it is required to investigate the dissolution/aggregation of other soluble metallic ENPs within a matrix of water properties mimicking natural conditions.

## Acknowledgements

The research described in this work was performed within the framework of the "NANOFASE" project supported by the European Union's Horizon 2020 research and innovation programme under grant agreement number 642007. M.G. Vijver was funded by the Dutch Organisation of Scientific Research (NWO) by the NWO-VIDI grant 864.13.010. D. Arenas-Lago would like to thank the Xunta de Galicia and the University of Vigo for the Postdoctoral grant (Ref. ED48 1B 2016/152-0).

## Appendix A. Supplementary data

Supplementary data to this article can be found online at https://doi.org/10.1016/j.chemosphere.2019.03.190.

## References

Abdolahpur Monikh, F., Praetorius, A., Schmid, A., Kozin, P., Meisterjahn, B., Makarova, E., Hofmann, T., von der Kammer, F., 2018. Scientific rationale for the development of an OECD test guideline on engineered nanomaterial stability. NanoImpact 11, 42–50. https://doi.org/10.1016/j.impact.2018.01.003.

Adeleye, A.S., Conway, J.R., Perez, T., Rutten, P., Keller, A.A., 2014. Influence of extracellular polymeric substances on the long-term fate, dissolution, and speciation of copper-based nanoparticles. Environ. Sci. Technol. 48, 12561–12568. https://doi.org/10.1021/es5033426.

Aiken, G.R., Hsu-Kim, H., Ryan, J.N., 2011. Influence of dissolved organic matter on the environmental fate of metals, nanoparticles, and colloids. Environ. Sci. Technol. 45, 3196–3201. https://doi.org/10.1021/es103992s.

Axson, J.L., Stark, D.I., Bondy, A.L., Capracotta, S.S., Maynard, A.D., Philbert, M.A., Bergin, I.L., Ault, A.P., 2015. Rapid kinetics of size and pH-dependent dissolution and aggregation of silver nanoparticles in simulated gastric fluid. J. Phys. Chem. C 119, 20632–20641. https://doi.org/10.1021/acs.jpcc.5b03634.

Chowdhury, I., Walker, S.L., Mylon, S.E., 2013. Aggregate morphology of nano-TiO2: role of primary particle size, solution chemistry, and organic matter. Environ. Sci. Process. Impacts 15, 275–282. https://doi.org/10.1039/c2em30680h.

Collins, D., Luxton, T., Kumar, N., Shah, S., Walker, V.K., Shah, V., 2012. Assessing the impact of copper and zinc oxide nanoparticles on soil: a field study. PLoS One 7. https://doi.org/10.1371/journal.pone.0042663.

Conway, J.R., Adeleye, A.S., Gardea-Torresdey, J., Keller, A.A., 2015. Aggregation, dissolution, and transformation of copper nanoparticles in natural waters. Environ. Sci. Technol. 49, 2749–2756. https://doi.org/10.1021/es504918q.

Flemming, C.A., Trevors, J.T., 1989. Copper toxicity and chemistry in the environment: a review. Water Air Soil Pollut. 44, 143–158. https://doi.org/10.1007/BF00228784.

Griffitt, R.J., Weil, R., Hyndman, K.A., Denslow, N.D., Powers, K., Taylor, D., Barber, D.S., 2007. Exposure to copper nanoparticles causes gill injury and acute lethality in zebrafish (Danio rerio). Environ. Sci. Technol. 41, 8178–8186. https://doi.org/10.1021/es071235e.

Gunsolus, I.L., Mousavi, M.P.S., Hussein, K., B?hlmann, P., Haynes, C.L., 2015. Effects of humic and fulvic acids on silver nanoparticle stability, dissolution, and toxicity. Environ. Sci. Technol. 49, 8078–8086. https://doi.org/10.1021/acs.est.5b01496.

Johnson, A.C., Bowes, M.J., Crossley, A., Jarvie, H.P., Jurkschat, K., Jürgens, M.D., Lawlor, A.J., Park, B., Rowland, P., Spurgeon, D., Svendsen, C., Thompson, I.P., Barnes, R.J., Williams, R.J., Xu, N., 2011. An assessment of the fate, behaviour and environmental risk associated with sunscreen TiO2nanoparticles in UK field scenarios. Sci. Total Environ. 409, 2503–2510. https://doi.org/10.1016/j.scitotenv.2011.03.040.

Jones, E.H., Su, C., 2012. Fate and transport of elemental copper (Cu0) nanoparticles through saturated porous media in the presence of organic materials. Water Res. 46, 2445–2456. https://doi.org/10.1016/j.watres.2012.02.022.

Kanel, S.R., Flory, J., Meyerhoefer, A., Fraley, J.L., Sizemore, I.E., Goltz, M.N., 2015. Influence of natural organic matter on fate and transport of silver nanoparticles in saturated porous media: laboratory experiments and modeling. J. Nanoparticle Res. 17. https://doi.org/10.1007/s11051-015-2956-y.

Keller, A.A., Wang, H., Zhou, D., Lenihan, H.S., Cherr, G., Cardinale, B.J., Miller, R., Zhaoxia, J.I., 2010. Stability and aggregation of metal oxide nanoparticles in natural aqueous matrices. Environ. Sci. Technol. 44, 1962–1967. https://doi.org/10.1021/es902987d.

Korshin, G.V., Frenkel, A.I., Stern, E.A., 1998. EXAFS study of the inner shell structure in copper(II) complexes with humic substances. Environ. Sci. Technol. 32, 2699–2705. https://doi.org/10.1021/es980016d.

Kosmulski, M., 2009. Compilation of PZC and IEP of sparingly soluble metal oxides and hydroxides from literature. Adv. Colloid Interface Sci. https://doi.org/10.1016/j.cis.2009.08.003.

Levard, C., Mitra, S., Yang, T., Jew, A.D., Badireddy, A.R., Lowry, G.V., Brown, G.E., 2013. Effect of chloride on the dissolution rate of silver nanoparticles and toxicity to E. coli. Environ. Sci. Technol. 47, 5738–5745. https://doi.org/10.1021/es400396f.

Levard, C., Reinsch, B.C., Michel, F.M., Oumahi, C., Lowry, G.V., Brown, G.E., 2011. Sulfidation processes of PVP-coated silver nanoparticles in aqueous solution: impact on dissolution rate. Environ. Sci. Technol. 45, 5260–5266. https://doi.org/10.1021/es2007758.

Li, X., Lenhart, J.J., Walker, H.W., 2012. Aggregation kinetics and dissolution of coated silver nanoparticles. Langmuir 28, 1095–1104. https://doi.org/10.1021/la202328n.

Li, X., Lenhart, J.J., Walker, H.W., 2010a. Dissolution-accompanied aggregation kinetics of silver nanoparticles. Langmuir 26, 16690–16698. https://doi.org/10.1021/la101768n.

Li, X., Lenhart, J.J., Walker, H.W., 2010b. Dissolution-accompanied aggregation kinetics of silver nanoparticles. Langmuir 26, 16690–16698. https://doi.org/10.1021/la101768n.

Linlin, Z., Tanaka, K., 2014. Dissolution of silver nanoparticles in presence of natural organic matter. Adv. Mater. Lett. 5, 6–8. https://doi.org/10.5185/amlett.2013.7520.

Louie, S.M., Spielman-Sun, E.R., Small, M.J., Tilton, R.D., Lowry, G.V., 2015. Correlation of the physicochemical properties of natural organic matter samples from different sources to their effects on gold nanoparticle aggregation in monovalent electrolyte. Environ. Sci. Technol. 49, 2188–2198. https://doi.org/10.1021/es505003d.

Misra, S.K., Dybowska, A., Berhanu, D., Luoma, S.N., Valsami-Jones, E., 2012. The complexity of nanoparticle dissolution and its importance in nanotoxicological studies. Sci. Total Environ. 438, 225–232. https://doi.org/10.1016/j.scitotenv.2012.08.066.

Mitrano, D.M., Ranville, J.F., Bednar, A., Kazor, K., Hering, A.S., Higgins, C.P., 2014. Tracking dissolution of silver nanoparticles at environmentally relevant concentrations in laboratory, natural, and processed waters using single particle ICP-MS (spICP-MS). Environ. Sci. Nano 1, 248–259. https://doi.org/10.1039/C3EN00108C.

Molleman, B., Hiemstra, T., 2017. Time, pH, and size dependency of silver nanoparticle dissolution: the road to equilibrium. Environ. Sci. Nano 4, 1314–1327. https://doi.org/10.1039/c6en00564k.

Mudunkotuwa, I.A., Pettibone, J.M., Grassian, V.H., 2012. Environmental implications of nanoparticle aging in the processing and fate of copper-based nanomaterials. Environ. Sci. Technol. 46, 7001–7010. https://doi.org/10.1021/es203851d.

Odzak, N., Kistler, D., Behra, R., Sigg, L., 2014. Dissolution of metal and metal oxide nanoparticles in aqueous media. Environ. Pollut. 191, 132–138. https://doi.org/10.1016/j.envpol.2014.04.010.

The Geochemical Atlas of Europe [WWW Document], n.D. URL http://weppi.gtk.fi/publ/foregsatlas/-ForegsData.php.

Vance, M.E., Kuiken, T., Vejerano, E.P., McGinnis, S.P., Hochella, M.F., Hull, D.R., 2015. Nanotechnology in the real world: redeveloping the nanomaterial consumer products inventory. Beilstein J. Nanotechnol. 6, 1769–1780. https://doi.org/10.3762/bjnano.6.181.

von der Kammer, F., Ferguson, P.L., Holden, P.A., Masion, A., Rogers, K.R., Klaine, S.J., Koelmans, A.A., Horne, N., Unrine, J.M., 2012. Analysis of engineered nanomaterials in complex matrices (environment and biota): general considerations and conceptual case studies. Environ. Toxicol. Chem. https://doi.org/10.1002/etc.723.

Von Der Kammer, F., Ottofuelling, S., Hofmann, T., 2010. Assessment of the physicochemical behavior of titanium dioxide nanoparticles in aquatic environments using multi-dimensional parameter testing. Environ. Pollut. 158, 3472–3481. https://doi.org/10.1016/j.envpol.2010.05.007.

Wagner, S., Gondikas, A., Neubauer, E., Hofmann, T., Von Der Kammer, F., 2014. Spot the difference: engineered and natural nanoparticles in the environment-release, behavior, and fate. Angew. Chem. Int. Ed. https://doi.org/10.1002/anie.201405050.

Wang, L.F., Habibul, N., He, D.Q., Li, W.W., Zhang, X., Jiang, H., Yu, H.Q., 2015. Copper release from copper nanoparticles in the presence of natural organic matter. Water Res. 68, 12–23. https://doi.org/10.1016/j.watres.2014.09.031.

Wang, Z., Li, J., Zhao, J., Xing, B., 2011. Toxicity and internalization of CuO nanoparticles to prokaryotic alga microcystis aeruginosa as affected by dissolved organic matter. Environ. Sci. Technol. 45, 6032–6040. https://doi.org/10.1021/es2010573.

Wang, Z., Zhang, L., Zhao, J., Xing, B., 2016. Environmental processes and toxicity of metallic nanoparticles in aquatic systems as affected by natural organic matter. Environ. Sci. Nano. https://doi.org/10.1039/c5en00230c.

Zhang, H., Chen, B., Banfield, J.F., 2010. Particle size and pH effects on nanoparticle dissolution. J. Phys. Chem. C 114, 14876–14884. https://doi.org/10.1021/jp1060842.

Zou, X., Li, P., Lou, J., Fu, X., Zhang, H., 2017. Stability of single dispersed silver nanoparticles in natural and synthetic freshwaters: effects of dissolved oxygen. Environ. Pollut. 230, 674–682. https://doi.org/10.1016/j.envpol.2017.07.007.